

# Atmospheric Nitrogen Plasma-Induced for Embedding NH<sub>2</sub>@Cubic-Bicontinuous Mesoporous Silica as Uranium (VI) Adsorbent Candidate in Seawater

N. S. Pamungkas<sup>1</sup>, D. Wongsawaeng<sup>1\*</sup>, D. Swantomo<sup>2</sup>,  
K. Kamonsuangkasem<sup>3</sup>, S. Chio-Srichan<sup>3</sup>

<sup>1</sup>Research Unit on Plasma Technology for High-Performance Materials Development, Department of Nuclear Engineering, Faculty of Engineering, Chulalongkorn University, Bangkok 10330, Thailand

<sup>2</sup>Polytechnic Institute Nuclear Technology, National Research, and Innovation Agency, Yogyakarta 55281, Indonesia

<sup>3</sup>Synchrotron Light Research Institute (Public Organization), 111 University Avenue, Muang District, Nakhon Ratchasima 30000, Thailand

## ARTICLE INFO

### Article history:

Received 10 February 2023

Received in revised form 8 November 2023

Accepted 27 March 2024

### Keywords:

Nitrogen plasma  
Cubic bi-continuous  
Mesoporous silica  
Amine-modified  
Uranium  
Adsorption

## ABSTRACT

This work aims to achieve interesting progress in uranium extraction by introducing a promising strategy that utilizes atmospheric nitrogen plasma-induced amine modification of CBC (Cubic Bi-continuous) material, providing a compelling pathway to enhance CBC's adsorption properties specifically for uranium harvesting. CBCs mesoporous silica samples were prepared by mixing the Pluronic F-127 as a template and TEOS (Tetraethyl Orthosilicate) as silica sources in the sol-gel process under acidic conditions. The obtained CBCs were treated using nitrogen plasma at room temperature (RT) under atmospheric pressure in a customized-borosilicate plasma reactor. Subsequently, the treated CBCs were grafted with amine groups. The final samples were characterized using SAXS (Small Angle Synchrotron X-ray Scattering) to determine the phase and structure, SEM-EDS (Scanning Electron Microscopy-Energy Dispersive Spectroscopy) analysis to quantify the presence of silica, oxygen, and embedded nitrogen, and Specific Surface Area (SSA) Analyzer using Brunauer-Emmett-Teller (BET) method to determine the specific surface area and pore size distribution. The SAXS profiles indicate that the obtained samples can be classified as CBCs Im3m mesoporous silica. The presence of silica, oxygen, and nitrogen was verified through SEM-EDS analysis, with approximate compositions of 36-37 %, 51-62 %, and 0.7-1.0 %, respectively. The use of SSA analysis further supported the findings, confirming the typical adsorption isotherm IV model. The specific surface areas were measured to be 371 m<sup>2</sup>/g for pure CBC, 573 m<sup>2</sup>/g for P1-CBC, and 607 m<sup>2</sup>/g for P2-CBC. The pore size distribution analysis revealed mesoporous characteristics within the material, with pore sizes ranging from 4 to 6.5 nm. On a batch laboratory scale, the material achieved the highest adsorption capacity of 15.68 mg-U(VI)/g-NH<sub>2</sub>@P1-CBC from natural seawater after 1 hour of contact time.

© 2024 Atom Indonesia. All rights reserved

## INTRODUCTION

Radioactive contamination, such as uranium, has attracted significant attention from researchers due to the release of uranium from processing plants

or nuclear reactor accidents, resulting in elevated uranium levels in water bodies [1]. Many findings from the previous reports regarding the elimination of uranium with many multiform adsorbents have been widely examined namely low-density polyethylene (LDPE) [2], polymer gel [3], activated carbon [4], and carbon nanofibers [5]. Although substantial progress has been made over several

\*Corresponding author.

E-mail address: doonyapong.w@chula.ac.th

DOI: <https://doi.org/10.55981/aij.2024.1301>

periods, the removal of uranium (VI) in seawater is still a challenge due to the presence of complex elements. To elevate the selectivity of uranium adsorption, it is essential to find a new adsorbent candidate.

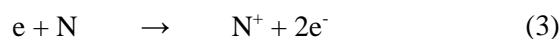
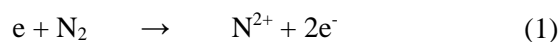
Mesoporous silica has been widely studied worldwide due to its characteristics. There are many kinds of mesoporous silica grouped into many kinds of shapes such as hexagonal, cubic, or lamellar. Cubic bi-continuous (CBC) mesoporous silica material has become interestingly developed. In previous findings study by Kleitz et al., the CBC mesoporous silica materials have a specific surface area (SSA) of up to 1000 m<sup>2</sup>/g [6]. SSA is one of the main essential characteristics of an adsorbent candidate. Besides, modification of surface site mesoporous could increase the adsorption performance. In seawater conditions, previous studies proved that the presence of primary amine could increase the uranium adsorption capacity [7-9].

Traditional methods for embedding amines onto the material have been explored by many researchers, including direct grafting [10] and co-condensation grafting methods [11]. However, in direct grafting, the mechanism by which a stable bond may be broken, and a carbon atom may not be replaced with a nitrogen atom, is observed during subsequent steps such as high-temperature calcination, leading to the degradation of amine groups [12]. To avoid those issues, a new pathway for attaching amines has recently been reported involving atmospheric nitrogen plasma, which enables the direct substitution of carbon with nitrogen on amorphous materials.

Plasmas are ionized gases and are also characterized as the fourth state of matter. They have a high level of energy, are reactive, and are responsive to electric and magnetic fields. Using nitrogen as feed in plasma, atomic nitrogen, and excited state molecules nitrogen in addition to negative ions can be produced. Due to those generated species, plasmas are important in the processing of materials, especially those used in surface modification [13]. Plasmas can also be used to improve the oxidation stability of biodiesel [14], control trans fatty acid margarine production [15], sterilize [16], catalyst modification [17], nanomaterials modification [18], wastewater treatment [19], and remove coronaviruses [20].

According to Ren et al.'s study, the N<sub>2</sub> gas injected into the plasma generator can be excited, and active nitrogen species (i.e., N\*) can be generated during the plasma discharge process [21]. During the initial stage, charged and neutral particles collide in the gas phase and with surfaces, limiting

the discharge and igniting recombination and neutralization reaction mechanisms. N<sub>2</sub> plasma species are generated, including N<sub>2</sub> molecules, molecular ions (N<sub>2</sub><sup>+</sup>), atomic species (N, N<sup>+</sup>), and radicals (N\*, N<sup>+\*</sup>). Nitrogen plasma was chosen because the process resulted in more nitrogen atoms in the treated mesoporous silica materials' hydrocarbon channel. Furthermore, nitrogen gas is abundant in the atmosphere and produces nontoxic active plasma species that can be used to modify surfaces [22]. The reactions of nitrogen plasma generating noble species are shown in chemical reactions from Eq. (1-3) below.



The plasma-induced grafting method is the prospective method to attach and modify the decoration of mesoporous silica with special functional groups. This method is predicted to have less environmental impact because no additional chemicals are used in the grafting process compared to the commercial grafting method. In summary, this method leads to more effective processes and fewer negative effects when grafting special groups without changing the raw material.

Porrang et al., study's findings revealed that the copper-coil Dielectric Barrier Discharge (DBD) plasma was successfully applied to graft vinyl groups onto mesoporous silica nanoparticles derived from rice husk, prepared as a drug delivery vehicle. The results showed that the drug vehicle-treated using plasma achieved a high level of apoptosis in the MCF-7 cells [5]. In another study, amidoxime was grafted to Carbon Nano Fibers (CNFs) using nitrogen plasma for 238U(VI) and 241Am(III) adsorption by Sun et al. [23].

Although several types of plasma generation have been discussed in previous research, there is no reference to the use of aluminum plate DBD nitrogen plasma in the modification of mesoporous silica CBC material, indicating that this proposed procedure has not been thoroughly investigated. This work has made significant advancements in the field of uranium extraction by introducing a promising new strategy. Firstly, a novel approach was proposed, involving the utilization of nitrogen plasma-induced amine modification of CBC (Cubic Bi-continuous) material. This innovative method presents an exciting avenue for enhancing the adsorption properties of CBC, specifically for uranium extraction purposes.

## METHODOLOGY

### Chemicals

The samples were prepared in this study using >99 % Tetraethyl orthosilicate (TEOS) from Sigma Aldrich, Pluronic F-127 from Sigma Aldrich as a CBC template, hydroxylamine hydrochloride (NH<sub>2</sub>OH.HCl) from KEMAUS as an amino source, methanol (CH<sub>3</sub>OH) from Sigma Aldrich, N-Butanol from Ajax Finechem, 37 % Hydrochloric acid (HCl) from QRec, ethanol (EtOH/C<sub>2</sub>H<sub>5</sub>OH) from Sigma Aldrich, Sodium Hydroxide 1M from KEMAUS, and DI water.

### Synthesis of cubic Bi-continuous

CBC samples were synthesized following the previous recipe from Pamungkas et al. [24]. The template was dissolved in DI water at RT. After the template was entirely dissolved, the co-template N-butanol (BuOH) was poured into the mixture at RT and stirred for 1 hour. Then, the silica source was added dropwise. After 1 h, an amino source was added to the solution and mixed at 45-50°C overnight. Thereafter, the solution was aged at 95-100°C for 24h with stirring. The resulting material was filtered and washed until a pH of 5-6. Calcination at 550°C for 6 hours was used to remove the template. The synthesized samples were noted as non-grafted CBC.

### Nitrogen plasma grafting procedure

One gram of non-grafted CBC was shined by nitrogen plasma in a customized borosilicate plasma reactor (10 x 10 x 6 cm) for 15 and 25 minutes. Figure 1 shows the nitrogen plasma treatment instrument setup. Nitrogen gas rate, pressure, power, voltage, and electrical current are 1 L/min, 100 kPa (1atm), 70W, 219-226V, and 0.311-0.344 mA, respectively. After the exposure to nitrogen plasma, the reactor was heated to 60°C, and a solution of 1.5M NH<sub>2</sub>OH.HCl (hydroxylamine) in 50/50 (v/v) % methanol/DI water solvent (pH=6-7; adjusted by KOH 1M) was injected and mixed under stirring for 5 h. The modified CBC was then filtered, washed with a mixture solution of EtOH (60 ml) and DI water (60 ml), and dried at 60°C overnight. The resulting modified material was donated as P1-CBC (25 minutes of plasma treatment) and P2-CBC (15 minutes of plasma treatment).

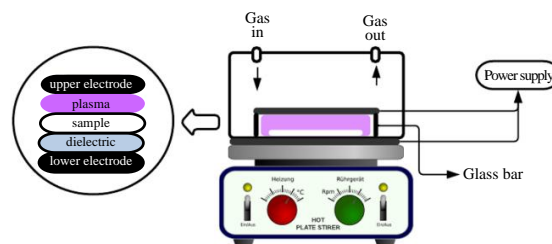


Fig. 1. Plasma treatment setup.

### Adsorption performance test

A sample of 50 ml natural seawater was prepared spiked with a uranium standard solution to achieve a concentration of 65.4 ppm at pH=6. After that, 0.1-0.2 grams of modified CBC was added to the solution with continuous stirring at RT for 1 h. The solution was then filtered, and the supernatant was analyzed using ICP-OES to determine the remaining uranium concentrations.

### Characterization of samples

#### Small angle synchrotron x-ray scattering (SAXS)

SAXS analysis of CBCs was performed at beamline BL1.3W at Synchrotron Light Research Institute (SLRI). Monochromatized X-ray with the energy 9 keV from brilliant synchrotron radiation at 1.2 GeV were directed onto the prepared CBC samples. The scattering profiles were recorded using a Rayonix SX165 CCD detector positioned at a sample-to-detector distance of 2.2 m. The resulting profiles covered a range of momentum transfer ( $q$ ) of  $0.5 < q < 2 \text{ nm}^{-1}$ . After that, the obtained data were processed and fitted using SAXSIT to obtain the scattering profile of CBCs samples.

#### Synchrotron radiation low-angle x-ray diffraction (SR-LXRD)

SR-LXRD was performed to study the amorphous phase of CBC materials at beamline BL1.1 at SLRI. The samples were irradiated using synchrotron radiation with an energy of 6 keV (CuK-Alpha) ( $\lambda=0.20664 \text{ nm}$ ) at  $0.5-2^\circ$  for 900 sec/sample. At the beginning of data processing, the collected data were subtracted from the background. The final data was presented in graphic 2 thetas versus diffraction intensity.

### Scanning electron microscopy-energy dispersive spectroscopy (SEM-EDS)

The number of silica, oxygen, and nitrogen elements in the decoration of modified CBC materials was also determined using SEM-EDS. SEM-EDS: FEI QUANTA 450-Oxford EDS XMax in Microscopy Laboratory at SLRI, was used to quantify the samples.

### Specific surface area analyzer (SSA)

SSA was performed to analyze the specific surface area, isotherm profile, and pore distribution of CBC material. Quanta chrome Autosorb 1-MP and Brunauer Emmett Teller (BET) were used to analyze the sample at Petroleum and Petrochemical College, Chulalongkorn University.

### Inductively coupled plasma-optical emissions spectrometry (ICP-OES)

The uranium concentration adsorbed in modified CBCs was determined using an ICP-OES. After the adsorption process, 10-15 ml of the supernatant solution was analyzed. The amount of uranium adsorbed in modified CBCs was calculated as the difference between the initial concentration of uranium and the concentration measured in the supernatant solution.

## RESULTS AND DISCUSSION

Figure 2 depicts the optical emission spectrum of nitrogen plasma. Optical Emission Spectroscopy (OES) is a non-destructive technique for studying the radicals' active species, atoms, and ions produced in plasma. In this study's results, the primary species identified in plasma are the N<sub>2</sub> second positive system (320, 340, and 360 nm) and the first negative system N<sup>2+</sup> (380 and 410 nm). The results confirmed that the samples were successfully bombarded by N<sup>2+</sup> ions during the plasma treatment, as previously reported by Hosseini et al. [25].

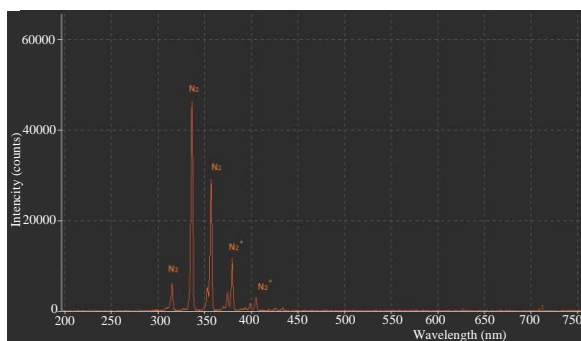


Fig 2. Optical emission of DBD nitrogen plasma and its active species.

The OES revealed that DBD N<sub>2</sub> plasma is a rich source of reactive nitrogen species and N<sub>2</sub> ions. Because of those reactive species, they can influence the structural arrangement of CBC material in many different ways, including physical modification, reactive chemical bonding, thermal induction, and interaction with UV radiation produced in plasma. The nitrogen-reactive species can participate in many chemical processes by expelling electrons and oxidizing materials. The placement of material in the cathode region, where electromagnetic power transmits to plasma, may increase the influence of those reactive ions and excited species. This effect can be observed in the physical change of the material's color from white to darker. Because plasma treatment was performed at atmospheric pressure in this study, it was essential to investigate the effect of the treatment time on the sample as well as the gap between the dielectric plate and the sample. By studying the effect of the gap between the upper electrode and the sample, the plasma did not appear when the gap was set higher and lower than 0.5 cm. Finally, in this study, it can be concluded that 0.5 cm of gap produces more homogeneous plasma.

Due to the presence of active nitrogen ions, SBA-16 material can be promptly activated during plasma treatment. The suggested mechanism of amine groups generated by N<sub>2</sub> plasma being grafted onto SBA-16 is depicted in Fig. 3. During the discharge of N<sub>2</sub> plasma, the active species of nitrogen ions (N<sup>\*</sup>) react with SBA-16 to produce active species (-O<sup>\*</sup>) on the surfaces and/or to replace the hydroxyl (-Si-OH) and siloxane (-Si-O-Si-) groups. Subsequently, amine groups were grafted onto the surface of SBA-16 after plasma activation through the oxygen-active species bond with the amine. The hydrophilic modification of the SBA-16 surfaces occurs as a result of the attack of active plasma species on the material and the incorporation of hydrophilic groups, including hydroxyl groups.

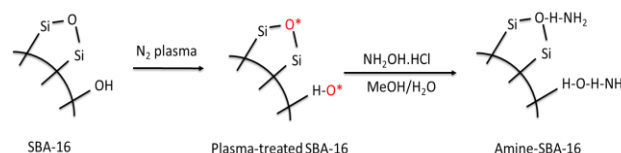


Fig. 3. Formation schematic of plasma grafting processes on SBA-16.

Nowadays, the application of non-destructive analysis by using X-rays has gradually been widely utilized by many researchers in the study and production of various disciplines. In this study, the utilized X-ray beam was produced by accelerating electrons to almost the speed of light known as

synchrotron radiation. As the electrons are deflected through magnetic fields, they produce extremely bright light. The intense light is channeled down the beamline to the experimental workstation, where it is used for research purposes such as XRD and SAXS. Both XRD and SAXS analysis in this study were performed at beamlines 1.1 and 1.3 of SLRI, respectively.

SAXS is one of the investigation tools to understand the structural properties in many mesoporous matter systems at length scales ranging from 1 to 100 nm using scattering of the incoming x-ray beam. The ordered CBC can be analyzed to generate different scattering momentum ( $q$ ) using SAXS profiles in the range of about  $0.5 < q < 2.0 \text{ nm}^{-1}$  shown in Fig. 4(a). The reflection of (110) planes could be identified by SAXS for all the samples. However, the P1-CBC sample exhibited a broad peak, and the number of  $q$  values tended to increase and shift significantly. It was predicted that the

higher exposure to nitrogen plasma resulted in a more pronounced arrangement of CBC crystal planes. By identifying the peak ratio of the recorded data, the synthesized materials can be categorized as Im3m cubic body-centered structures [26,27].

X-ray diffraction analysis is used to provide valuable information about the structure and properties of a material by analyzing the diffraction of incoming X-ray beam. This was verified experimentally and a defined arrangement of atoms in the crystal was established. In Fig. 4(b), the XRD patterns of the synthesized samples are shown. Consistent with the SAXS results, the XRD pattern of the P1-CBC sample showed a broad diffraction peak. A major diffraction peak of the XRD patterns could be indexed to the amorphous cubic body-centered space group Im3m [24,28]. Because P1-CBC was predicted to have homogeneously nitrogen distribution, the adsorption performance also recorded higher uptake of uranium (see Table 1).

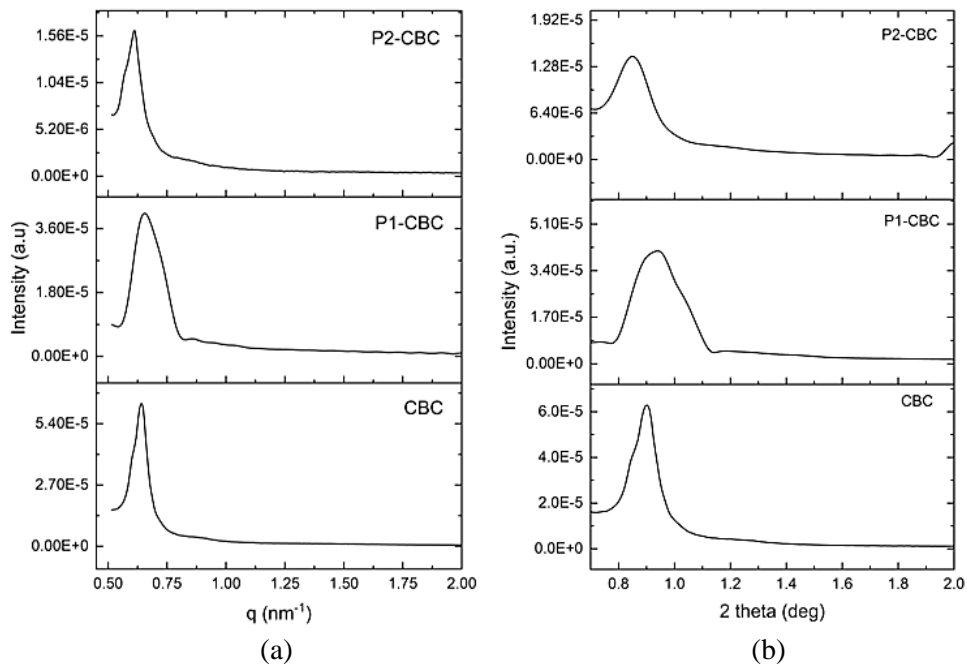


Fig. 4. (a) SAXS and (b) XRD profiles of CBC materials.

Table 1. Summarize of adsorption test and related uranium adsorption studies.

Sample Code	Conditions	Uranium Adsorbed (mg-U/g-ads)	Remark
CBC	Initial uranium concentration: 65.4 ppm; room temperature; pH:6-7; non-plasma; non-grafted; reaction time:1 h, natural seawater, no amine ligands.	9.50	This work
P1-CBC	Initial uranium concentration: 65.4 ppm; room temperature; pH:6-7; plasma treatment at 70 W of power, 226 Volt of Voltage; 0.344 A of Current; treatment time: 25 mins; amine concentration: 1.27 M; adsorption time: 1 h, natural seawater, amine ligands.	15.68	This work
P2-CBC	Initial uranium concentration: 65.4 ppm; room temperature; pH:6-7; plasma treatment at 70 W of power, 219 Volt of Voltage; 0.311 A of Current; treatment time: 15 mins; amine concentration: 1.27 M; adsorption time: 1 h, natural seawater, amine ligands.	7.86	This work
Magnetic Fe <sub>3</sub> O <sub>4</sub>	Initial uranium concentration: 30 mg/L; T:293.15 K; pH: 6; RF (Radio Frequency) plasma; plasma treatment at 100 W of power, treatment time: 120 min; adsorption time: 1 h, amines ligands, simulated wastewater.	228.17	[33]
Carbon nanotubes	Initial uranium concentration: 1000 mg/L; T:293.15 K; pH: 4.5; Nitrogen plasma; plasma treatment at 100 W of power, pressure: 10 Pa; Voltage: 800 V; electrical current: 15 mA; treatment time: 40 min; adsorption time: 0.5 h, simulated nuclear industry effluent, amidoxime ligands.	145	[34]
Mesoporous carbon CMK-5	Initial uranium concentration: 100 mg/L, pH: 5, T:283.15 K, adsorption time: 2 h, non-plasma treatment, simulated nuclear industry effluent, oxime ligands.	45	[35]
Amidoxime-modified fiber adsorbent	Adsorption parameter: (a) T: 15-30°C, adsorption time: 2 hours to 240 days, amidoxime ligand, uranium in seawater.	0.1-3.2	[36]

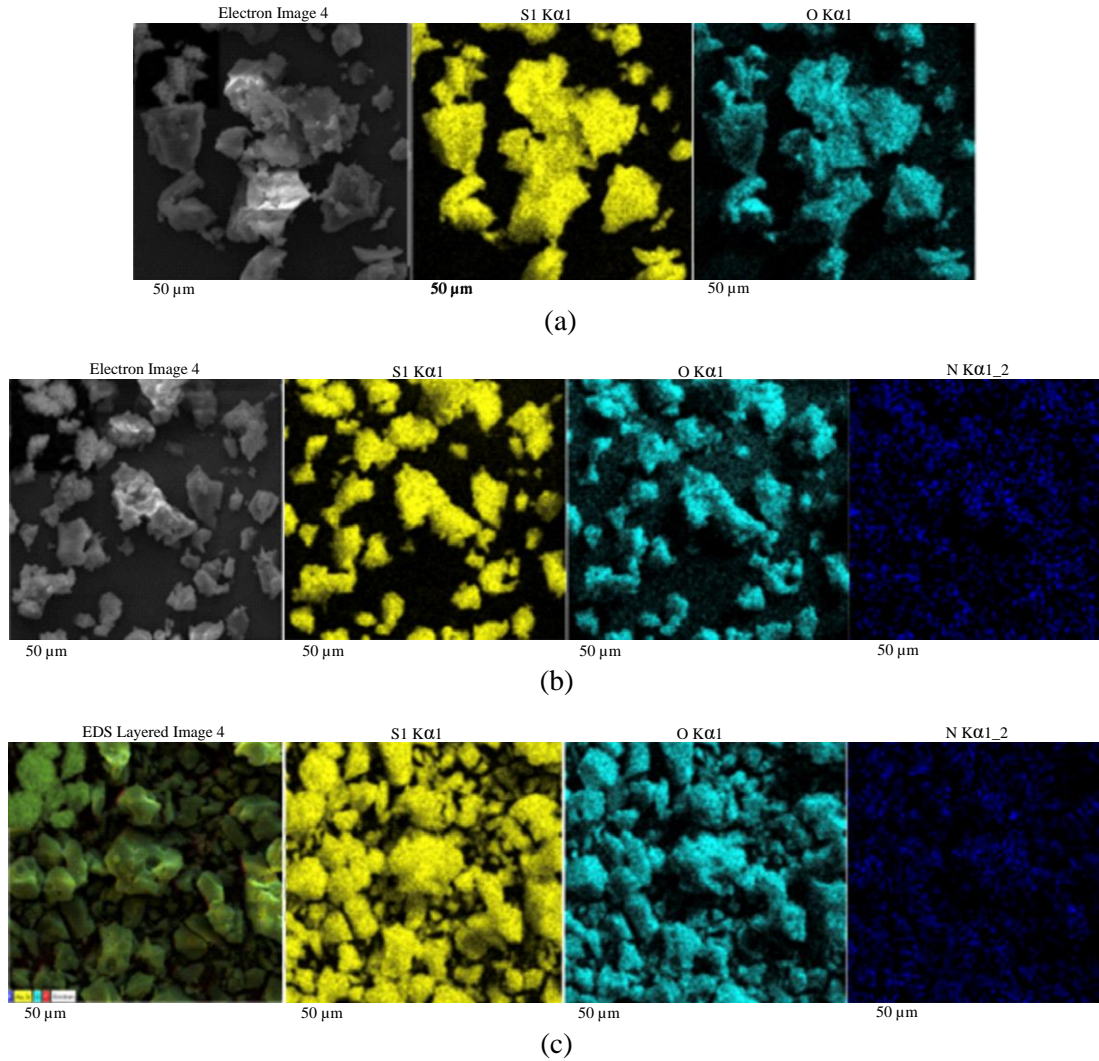


Fig. 5. Images of element mapping of CBC material (a) CBC, (b) P1-CBC, and (c) P2-CBC.

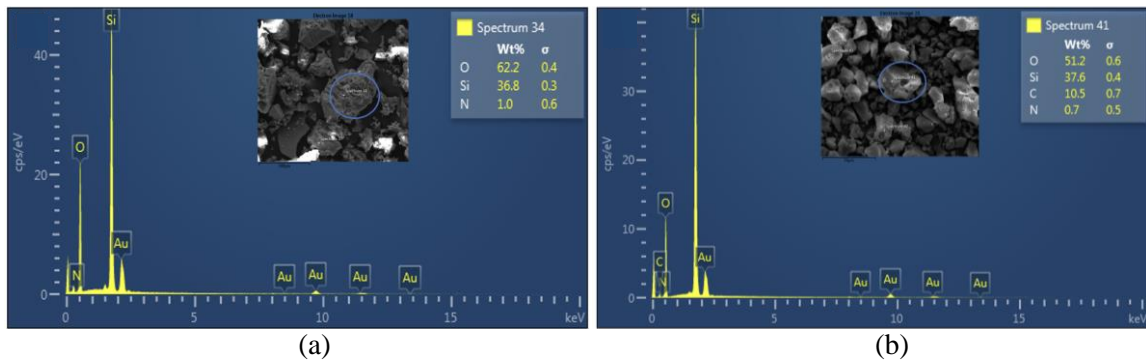


Fig. 6. EDS of (a) P1-CBC and (b) P2-CBC samples.

Figure 5 presents SEM images and element distribution map of all samples obtained using mapping EDS. It was recorded that the pure CBC did not detect nitrogen elements. However, nitrogen elements were detected after plasma grafting on the surface of CBC. Figure 6 shows the emissions spectra for the materials P1-CBC and P2-CBC, which contain embedded amine. It was observed that silica (Si) dominated the spectra, rather than oxygen (O) and nitrogen (N).

The EDS result of the P1-CBC sample revealed higher nitrogen distribution than the P2-CBC sample shown in Fig. 6. Nitrogen plasma contains reactive species that can participate in etching and burning-up effects. It is believed that the reactive plasma species modify the surface groups of CBC materials [29]. This finding is consistent with the previous study by Li et al., which demonstrated that plasma-treatment time can influence the decoration functional groups of material [29]. Quantitative data of nitrogen elements

from EDS results successfully proved that plasma grafting is a potential method for grafting amine groups in the CBC materials. After the de-templating process, there are carbon species in the P2-CBC sample that were predicted from the template residual. This result aligns with earlier research by Basso et al., which revealed that for synthesized samples, 0.32-0.42 % of the carbon remained following a 5-hour de-templating process [30].

Based on the characterization of CBC material, the P1-CBC sample has the best feature of amine-modified CBC material using atmospheric nitrogen plasma. As a result, the materials performed nitrogen isotherm adsorption. According to the IUPAC classification standard [31], the isotherm profile shown in Figs. 7(a-c) is a typical type IV

isotherm, indicating that the sample is mesoporous. At P/P0=0.4-0.7, the framework confined mesopores filled. Furthermore, the sample's pore diameter distribution range was 3-4 nm as shown in Figs. 7(d-f), with its specific surface area was 371 (CBC), 573 (P1-CBC), and 607 (P2-CBC) m<sup>2</sup>/g. However, the P2-CBC sample showed a high specific surface area (607 m<sup>2</sup>/g) and pore size distribution of 4-6.5 nm. This indicates that heat generation from plasma treatment is an effective pretreatment method for increasing specific surface area and pore distribution as physical characteristics of mesoporous silica. The finding is in the same agreement with the previous study about steam explosion treatment on bagasse affecting the specific surface area and grafting ratio by Liang et al. [32].

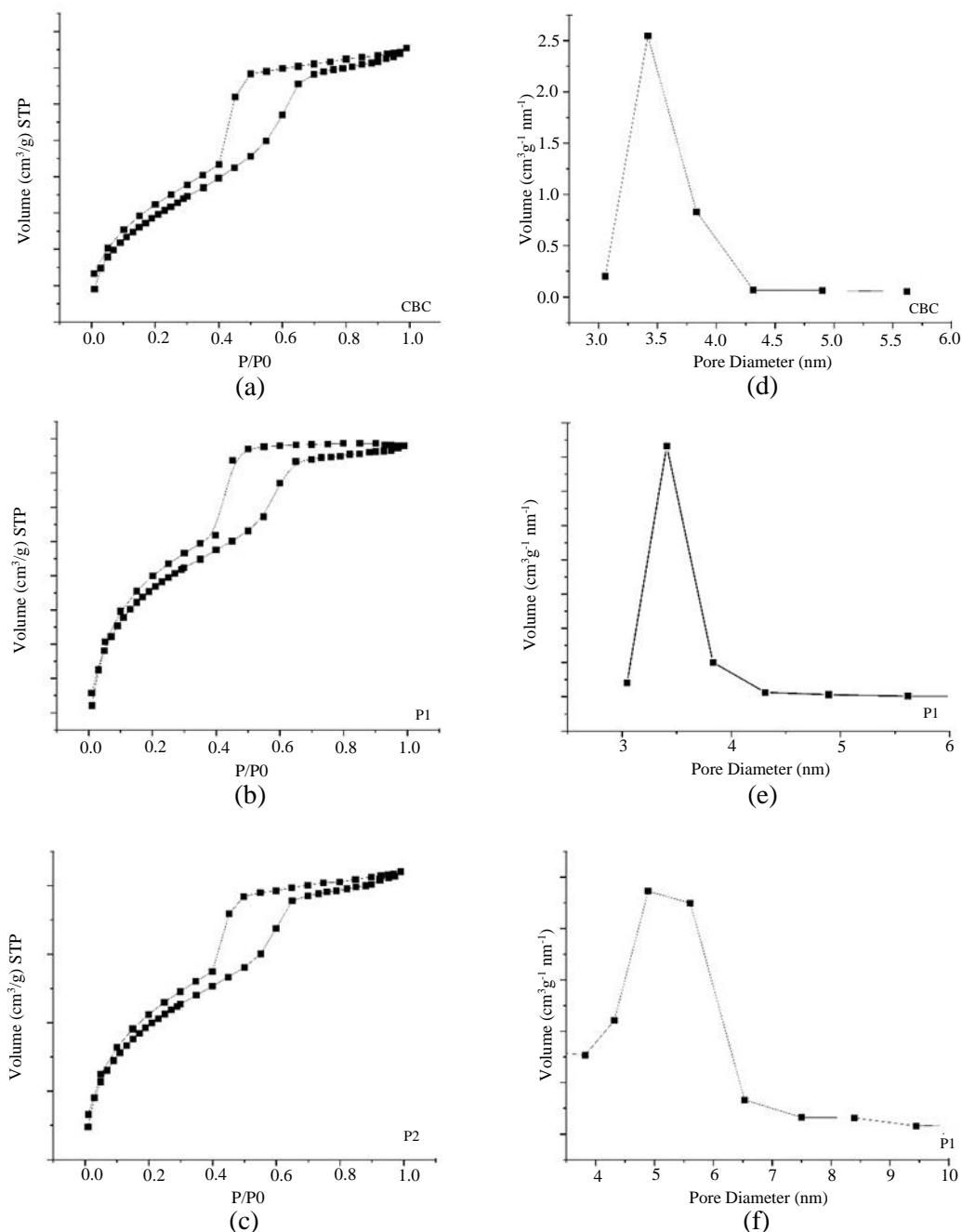
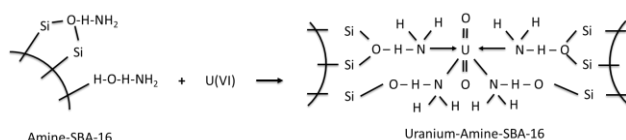


Fig. 7. (a-c) Nitrogen adsorption isotherm profile; (d-f) Pore distribution of samples.



**Fig. 8.** Probable adsorption mechanism of uranium (VI) on SBA-16-NH<sub>2</sub>.

According to the probable method illustrated in Fig. 8, the amine groups of the amidoxime grafted SBA-16 through nitrogen plasma treatment are expected to adsorb uranium (VI). This is supported by previous studies, which revealed that the adsorption mechanism of the U(VI) involves complexation between the -H-NH<sub>2</sub> and =OH groups [37]. Amidoxime groups and uranium species have complex binding chemistry, as demonstrated by the binding of uranyl ions with two oxygen atoms from an amidoxime ligand and two oxygen atoms from an amidoxime anion, as well as the binding of oxygen (O) and nitrogen atoms (-NH<sub>2</sub>) from an amidoxime anion to form a ring structure.

By comparing all samples in the adsorption performance test, the highest uranium uptake was obtained by using the P1-CBC sample shown in Table 1. However, the results of this study revealed that the capacity of uranium adsorption was lower than in previous plasma treatment studies. It is essential to consider the experimental condition. Previous studies [26,27] utilizing plasma treatment employed a vacuum system and operated at low pressure, whereas this current study appears to have had a simpler instrument setup. Furthermore, the selection of the DBD (Dielectric Barrier Discharge) nitrogen plasma sandwich setup was based on several advantageous factors. Firstly, this configuration is known for its ability to generate and ensure that the plasma interacts uniformly with the powder [38], which is crucial for achieving consistent and reliable results. The sandwich design, with the powdered sample securely positioned between two dielectric barriers, prevents scattered samples. Moreover, their study was conducted in simulated nuclear industry effluent which contains higher uranium concentration than in seawater (around 3 ppb) and there are no impurities that disturbed the adsorption process [39].

According to the study review by Kim et al., uranium adsorption from seawater using amidoxime-modified fiber adsorbent reported capacities ranging from 0.1-3.2 mg-U/g-ads, based on contact time ranging from 2 hours to 240 days [36]. Three prepared samples reported 5-156 times higher uranium capacity when compared to this study. Seawater is a heterogeneous mixture of 96.5 %

water, 2.5 % salt, and minor quantities of other substances such as inorganic and organic matter, and particulates [40]. Due to these conditions, it was predicted that the adsorption process in natural seawater is more challenging. The biofouling agents and small matters may block or occupy the functional groups, reducing the availability for desired elements such as uranium. As a result, the number of adsorbed elements in natural seawater is smaller than in synthetic or man-made seawater [41,42]. In summary, this study suggests that atmospheric nitrogen plasma could be a promising method to prepare amine-modified CBC mesoporous material and harvest uranium from natural seawater.

## CONCLUSION

NH<sub>2</sub>@CBC material as an adsorbent candidate for uranium (VI) was successfully synthesized using atmospheric plasma induced in the customized-borosilicate reactor. SAXS and nitrogen adsorption isotherm type-IV profiles proved the Im3m mesoporous phase of CBC material. The CBC-treated (P1-CBC) atmospheric nitrogen plasma was recorded in 25 minutes resulting in the highest uranium intake from real seawater in the batch adsorption system. The highest uranium intake was around 15.68 mg-U/g-NH<sub>2</sub>@P1-CBC in 1 hour of adsorption time. Adjustments in plasma conditions result in different material characteristics. These findings highlight the successful synthesis and characterization of cubic bi-continuous Im3m mesoporous silica materials. The promising atmospheric nitrogen plasma grafting method employed in the synthesis of this material not only enhances material performance but also offers scalability and practicality for other elemental adsorption applications in the future. Further investigations into plasma parameter optimization are needed.

## ACKNOWLEDGMENT

The authors thank the financial support provided by The Scholarship from the Graduate School, Chulalongkorn University to commemorate the 72nd anniversary of His Majesty King Bhumibol Adulyadej, The Scholarship for Domestic Presentation from the Graduate School, Chulalongkorn University, Beamline 1.1 Multiple X-ray Techniques (X-ray Diffraction), and Beamline 1.3 Small and Wide-Angle X-ray Scattering, SLRI.



## AUTHOR CONTRIBUTION

N. S. Pamungkas, D. Wongsawaeng, and D. Swantomo equally contributed to the conceptualization, methodology, and investigation of this paper. K. Kamongsuangkasem and S. Chio-Srichan provided the synchrotron XRD and SAXS analysis tools, data processing, and assistance. All authors contributed writing, reviewing, and editing the final version of the paper.

## REFERENCES

1. T. P. Gandhi, P. V. Sampath and S. M. Maliyekkal, *Sci. Total Environ.* **825** (2022) 153947.
2. V. Ratnitsai, W. Wongjaikham, D. Wongsawaeng *et al.*, *J. Nucl. Sci. Technol.* **59** (2022) 629.
3. W. Wongjaikham, D. Wongsawaeng and P. Hosemann, *J. Nucl. Sci. Technol.* **56** (2019) 541.
4. A. Saputra, D. Swantomo, T. Ariyanto *et al.*, *Water Air Soil Pollut.* **230** (2019) 213.
5. S. Porrhng, N. Rahemi, S. Davaran *et al.*, *J. Taiwan Inst. Chem. Eng.* **123** (2021) 47.
6. F. Kleitz, S. H. Choi and R. Ryoo, *Chem. Commun.* **17** (2003) 2136.
7. Y. Guo, M. Xia, K. Shao *et al.*, *Phys. Chem. Chem. Phys.* **24** (2022) 17163.
8. M. Chaudhary, L. Singh, P. Rekha *et al.*, *Chem. Eng. J.* **378** (2019) 122236.
9. A. Najah, D. Boivin, C. Noël *et al.*, *Mater. Chem. Phys.* **290** (2022) 126629.
10. A. A. Hussain, S. Nazir, R. Irshad *et al.*, *Mater. Res. Bull.* **133** (2021) 111059.
11. S. M. Hafezian, P. Biparva, A. Bekhradnia *et al.*, *Adv. Powder Technol.* **32** (2021) 779.
12. M. Barczak, *New J. Chem.* **42** (2018) 4182.
13. F. F. Chen, *Introduction to plasma physics*, Springer Science & Business Media, New York (2012) 4.
14. G. Kongprawes, D. Wongsawaeng, P. Hosemann *et al.*, *Int. J. Energy Res.* **45** (2021) 4519.
15. K. Puprasit, D. Wongsawaeng, K. Ngaosuwan *et al.*, *Innovative Food Sci. Emerg. Technol.* **66** (2020) 102511.
16. Y. Todorova, E. Benova, P. Marinova *et al.*, *Processes* **10** (2022) 554.
17. Z. Ye, L. Zhao, A. Nikiforov *et al.*, *Adv. Colloid Interface Sci.* **308** (2022) 102755.
18. J. He, X. Wen, L. Wu *et al.*, *TrAC, Trends Anal. Chem.* **156** (2022) 116715.
19. H. Zeghioud, P. Nguyen-Tri, L. Khezami *et al.*, *J. Water Process Eng.* **38** (2020) 101664.
20. D. Ghernaout and N. Elboughdiri, *Open Access Lib. J.* **7** (2020) 1.
21. X. Ren, D. Shao, G. Zhao *et al.*, *Plasma Processes Polym.* **8** (2011) 589.
22. L. Wu, Y. Cai, S. Wang *et al.*, *Int. J. Hydrogen Energy* **46** (2021) 2432.
23. Y. Sun, S. Lu, X. Wang *et al.*, *Environ. Sci. Technol.* **51** (2017) 12274.
24. N. S. Pamungkas, D. Wongsawaeng, D. Swantomo *et al.*, *Eng. J.* **27** (2023) 45.
25. S. I. Hosseini, S. Mohsenimehr, J. Hadian *et al.*, *Phys. Plasma.* **25** (2018) 013525.
26. S. Banafti, M. Jahanshahi, M. Peyravi *et al.*, *Microporous Mesoporous Mater.* **299** (2020) 110107.
27. M. E. Adrover, M. Pedernera, M. Bonne *et al.*, *Saudi Pharm. J.* **28** (2020) 15.
28. S. Manimaran, K. Subramanian, R. Tschentscher *et al.*, *J. Porous Mater.* **29** (2022) 357.
29. K. Li, G. Liu, C. Wang *et al.*, *Catal. Commun.* **144** (2020) 106093.
30. A. M. Basso, B. P. Nicola, K. Bernardo-Gusmao *et al.*, *Appl. Sci.* **10** (2020) 970.
31. J. P. Ruelas-Leyva, L. F. Maldonado-Garcia, A. Talavera-Lopez *et al.*, *Catal.* **11** (2021) 128.
32. L. Liang, J. Li, J. Zeng *et al.*, *Bioresour.* **11** (2016) 6185.
33. S. Duan, X. Xu, X. Liu *et al.*, *J. Colloid Interface Sci.* **513** (2018) 92.
34. Y. Wang, Z. Gu, J. Yang *et al.*, *Appl. Surf. Sci.* **320** (2014) 10.
35. G. Tian, J. Geng, Y. Jin *et al.*, *J. Hazard. Mater.* **190** (2011) 442.
36. J. Kim, C. Tsouris, R. T. Mayes *et al.*, *Sep. Sci. Technol.* **48** (2013) 367.
37. Y. Tian, Y. Wang, L. Liu *et al.*, *J. Mol. Liq.* **372** (2023) 121171.

38. W. Wongjaikham, D. Wongsawaeng, K. Ngaosuwan *et al.*, *Eng. J.* **27** (2023) 1.
39. Y. Zhao, X. Hu, C. Shi *et al.*, *Constr. Build. Mater.* **295** (2021) 123602.
40. Z. Huang, H. Dong, N. Yang *et al.*, *ACS Appl. Mater. Interfaces* **12** (2020) 16959.
41. H. Yang, X. Liu, M. Hao *et al.*, *Adv. Mater.* **33** (2021) 2106621.
42. A. I. W. S. Ramadani, N. S. Pamungkas, N. A. Putrisetya *et al.*, *Atom Indones.* **46** (2020) 11.